13th IEA Heat Pump Conference
April 26-29, 2021 Jeju, Korea

Theoretical Analysis of Mass Transfer in a Vacuum Membrane Dehumidification System

Hye-Jin Cho[a], Seong-Yong Cheon[a], Su Liu[a], Jae-Weon Jeong[a*]

[a]Department of Architectural Engineering, College of Engineering, Hanyang University, Seoul, 04763, Republic of Seoul

Abstract

This paper theoretically investigated the dehumidification performance of a vacuum membrane dehumidification system. Dehumidification effectiveness and the coefficient of performance (COP) were adopted as measures of performance. A one-dimensional numerical model was developed to analyze the mass transfer in a membrane dehumidifier module as a function of variation of four operating parameters: the inlet air temperature, humidity ratio, velocity, and the pressure in the vacuum side. Parametric analysis of the proposed model demonstrated that the inlet air velocity and the pressure in the vacuum side significantly affected dehumidification performance. When the pressure in the vacuum side decreased from 101.3 to 1.0 kPa, the dehumidification effectiveness increased from 2.1 to 54.1 %, while the COP decreased from 23.9 to 1.7. Similarly, the dehumidification effectiveness decreased from 73.9 to 15.8 % and the COP increased from 1.9 to 2.5 with an increase in air velocity from 0.1 to 2.0 m/s. In addition, the energy performance of the proposed vacuum membrane dehumidification system in building application was evaluated by comparing with a conventional cooling coil system.

Selection and/or peer-review under responsibility of the organizers of the 13th IEA Heat Pump Conference 2020.

Keywords: vacuum membrane dehumidification; isothermal dehumidification; numerical simulation; air conditioning;

1. Introduction

To provide a suitable indoor environment to building occupants, the temperature and humidity of air inducted from the outside into buildings should be controlled. For decades, vapor compression-based air conditioning systems have been widely adopted in air conditioning systems since they are highly effective and convenient in operation. However, vapor compression air conditioning systems may have energy penalty because of the overcooling and reheating of the process air [1]. Desiccant-assisted systems have been suggested as an alternative option for dehumidification in air conditioning applications [2]. A desiccant absorbs moisture when a water vapor pressure difference exists between the process air and desiccant. Consequently, the desiccant system does not require the supply of overcooling and reheating energy. However, regeneration of the desiccant material results in considerable energy consumption if there are no free-heat sources.

Vacuum membrane-based dehumidification systems have been suggested in recent years as an alternative to vapor compression and desiccant-based dehumidification systems [3,4]. The membrane is made of hydrophilic and polymeric materials for transferring water vapor across the membrane. In a vacuum membrane dehumidification system, the main driving force for the transfer of moisture is the pressure difference across the membrane. Water vapor in the humid process air is absorbed and diffuses through the membrane owing to the pressure difference, which is generated by a vacuum pump depressurizing the permeate side. Water vapor that has penetrated to the permeate side is exhausted externally. Accordingly, the vacuum membrane dehumidification system can isothermally remove the latent load in the process air, and does not require heating or cooling during dehumidification.

* Corresponding author. Tel.: +82-2-2220-2370; fax: +82-2-2220-1945.
E-mail address: jjwarc@hanyang.ac.kr (J.-W. Jeong).

Several studies have investigated the potential of vacuum membrane dehumidification systems as a function of the membrane's material and configuration under various operating conditions [5–7]. However, research that addresses the operating conditions and workable design of a vacuum membrane dehumidifier remain very rare.

This study suggested the operating conditions and configuration of a vacuum membrane dehumidifier based on the results of a theoretical analysis. A one-dimensional numerical model for a vacuum membrane dehumidifier is derived, and the sensitivity of dehumidification performance to each operating parameter was analyzed by using the proposed model. The dehumidification and energy performance of the proposed system were evaluated by comparing it with a conventional vapor compression-based dehumidification system.

2. Vacuum membrane dehumidification system

2.1. System overview

In a vacuum membrane-based dehumidification system, dehumidification occurs by the vapor pressure difference between the feed side (or primary air side) and the permeate side (or secondary air side), which is separated by a dense hydrophilic membrane (Fig. 1). During dehumidification, water vapor in the feed side diffuses on the membrane and is transferred to the permeate side, and is then exhausted to the outside by a vacuum pump. The key function of the membrane is selective gas separation. In membrane-based gas separation, a membrane is characterized by its permeance, that is, the amount of a species passing through the membrane per unit area and unit pressure difference, and by its selectivity, the ratio of the amount of a species passing through membrane to that of other species [7]. Therefore, the permeability and the selectivity of the membrane to water vapor have significant impacts on the performance of the vacuum membrane dehumidification system.

In this study, a hollow fiber polyamide membrane coated with carboxylated titanium dioxide (C-TiO_2) nanoparticles dehumidifier was adopted. This membrane has a water vapour permeance of 4.68×10^{-7} mol/s m^2Pa and a selectivity of 510 for water vapor/dry air [3]. The thickness of membrane was 150 μm, and the inner and outer diameters of the hollow fiber were 480 μm and 685 μm, respectively. The outer diameter of the membrane module was 0.2 m. The number of hollow fibers in the membrane modules was set at 30,000.

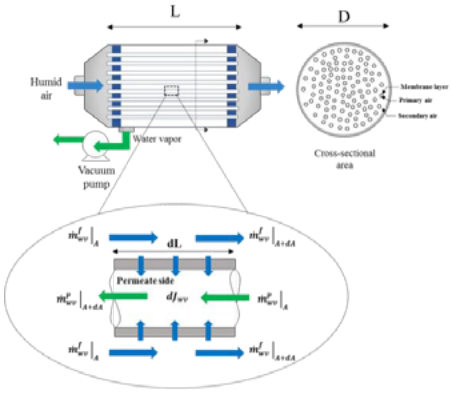

Fig. 1. Schematic of a vacuum membrane dehumidification system.

2.2. Numerical model derivation

In this study, it was assumed that mass transfer occurred along the direction of air flow (i.e. x-axis), from *x=0 to x=L*, and the water vapor transferred to the permeate side was exhausted in the opposite direction, from *x=L to x=0*, by the vacuum pump (Fig. 1). Other assumptions are as follow:

1. Dehumidification occurs under ideal gas conditions.
2. Dehumidification occurs in a steady state.
3. The permeability and selectivity are constant.
4. The process air only consists of water vapor and dry air.
5. The total air pressure from feed and permeate sides remain constant.
6. The initial water vapor pressure in permeate side is zero, the initial dry air pressure in permeate side is equal to the total vacuum side pressure.

2.3. Overall mass transfer coefficient

The simulation model in this work mainly consists of an overall mass transfer coefficient model and the mass balance equations between the air in feed side and permeate sides. In the overall mass transfer coefficient model, the convection-based mass transfer of the boundary layer of feed/permeate sides, and the permeance of the membrane to water vapor was considered. In addition, the overall mass resistance of the dry air should be considered in the performance of a vacuum membrane dehumidification system. Therefore, the overall mass transfer resistance of water vapor ($R_{t,wv}$) and dry air ($R_{t,da}$) can be estimated by the mass transfer resistance of water vapor ($R_{diff,wv}$) and dry air ($R_{diff,da}$), the mass resistance of the boundary layer in the feed side (R_{bl}^{f}) and permeate sides (R_{bl}^{p}) (Eqs. 1 and 2):

$$R_{t,wv} = R_{diff,wv} + R_{bl}^{f} + R_{bl}^{p} \tag{1}$$

$$R_{t,da} = R_{diff,da} + R_{bl}^{f} + R_{bl}^{p} \tag{2}$$

The overall mass resistance of the boundary layer can be estimated by Eq.3 with the molar density (ρ), and the mass transfer coefficient at the boundary layer (k_{bl}), which is defined by Eq. 4:

$$R_{bl} = \frac{1}{\rho k_{bl}} \tag{3}$$

$$k_{bl} = \frac{D_w \cdot Sh}{D_h} \tag{4}$$

where D_w is the diffusivity of water vapor in air, *Sh* is the Sherwood dimensionless number, and D_h is the hydraulic diameter of the fiber module. In this study, the *Sh* is defined by an empirical model, including the Reynolds (*Re*) and Schmidt (*Sc*) numbers (Eq.5), as suggested by Wang et al. [8]:

$$Sh = 0.3 + (0.62 Re_a^{0.5} \frac{Sc_a^{\frac{1}{3}}}{(1+(\frac{0.4}{Sc_a})^{\frac{2}{3}})^{\frac{1}{4}}} \cdot (1 + \frac{(\frac{Re_a}{282000})^5}{8})^{4/5} \tag{5}$$

In terms of the mass transfer coefficient of the dense membrane, the overall mass transfer resistance can be calculated from the membrane's thickness (δ_m) and water vapor permeance (Per_{wv}) (Eq. 6):

$$R_{diff,wv} = \frac{1}{Per_{wv}} \tag{6}$$

In addition, the overall mass transfer resistance of the dry air can be obtained if the water vapor permeance and the water vapor/dry air selectivity are known (Eq. 7):

$$Per_{da} = \frac{Per_{wv}}{Sel} \tag{7}$$

2.4. Mass balance equations

The mass balance of the water vapor in the feed/permeate sides can be written by the governing equations for the mass flux of water vapor (Eqs. 8 and 9):

$$\frac{dJ_{wv}}{dA} = \frac{(P^f_{wv} - P^p_{wv})}{R_{t,wv}} \tag{8}$$

$$dA = n_{fiber} \cdot \pi \cdot d_{i,f} \cdot dx \tag{9}$$

Where dJ_{wv}/dA indicate the mass flux of water vapor for the superficial surface area of each fiber module (dA), which can be obtained from the number of hollow fibers, the inner fiber diameter and fiber length. The total water vapor mass flow rate in feed/permeate sides after passing through the membrane can be estimated from the calculated mass flux for water vapor for each module (Eqs. 10 and 11):

$$\dot{m}^f_{wv}\big|_{A+dA} = \dot{m}^f_{wv}\big|_A - dJ_{wv} \tag{10}$$

$$\dot{m}^p_{wv}\big|_{A+dA} = \dot{m}^p_{wv}\big|_A + dJ_{wv} \tag{11}$$

Where $\dot{m}^f_{wv}$ and $\dot{m}^p_{wv}$ is the mass flow rate of water vapor of the feed/permeate sides and the pressure of the water vapor in feed/permeate sides can be obtained from Dalton's law of partial pressures for an ideal gas. The total dry air vapor mas flow rate in feed/permeate sides can also be obtained with the same method (Eqs. 12 and 13):

$$\dot{m}^f_{da}\big|_{A+dA} = \dot{m}^f_{da}\big|_A - dJ_{da} \tag{12}$$

$$\dot{m}^p_{da}\big|_{A+dA} = \dot{m}^p_{da}\big|_A + dJ_{da} \tag{13}$$

Then, the outlet air humidity ratio can be obtained from the pressure of the water vapor and dry air of the feed side (Eq. 14).

$$\omega_{a,out} = 0.622 \frac{P^f_{wv,out}}{P^f_{da,out}} \tag{14}$$

The differential elements of the computational domain can be expressed as *dx=L/N* when the domain is discretized by dividing the module length *L* (*x-axis*) into N segments. In this work, the domain was divided into 20 along the *x-axis*. Therefore, the governing equations for calculating the mass flux of the water vapor can be expressed the following discretized form (Eqs. 15–18):

$$J_{wv}[i+1] - J_{wv}[i] = \frac{\left(P^f_{wv}[i] - P^p_{wv}[i]\right)}{R_{t,wv}} \left(n_{fiber} \cdot \pi \cdot D_{i,f} \cdot \frac{L}{N}\right) \tag{15}$$

$$\dot{m}^f_{wv}[i+1] = \dot{m}^f_{wv}[i] - (J_{wv}[i+1] - J_{wv}[i]) \tag{16}$$

$$\dot{m}^p_{wv}[i+1] = \dot{m}^p_{wv}[i] + (J_{wv}[i+1] - J_{wv}[i]) \tag{17}$$

$$\omega_a[i+1] = 0.622 \frac{P^f_{wv}[i+1]}{P^f_{da}[i+1]} \tag{18}$$

The mass flux of dry air also can be calculated the same way. The gradients of humidity ratio in feed side in each segment can be estimated when the following boundary conditions are given: the initial water vapor/dry air pressure in the feed side, calculated from the inlet air temperature and humidity ratio, the mass resistance in the feed side boundary layer, calculated from the inlet velocity, and the vacuum side total pressure.

3. Simulation results

Dehumidification effectiveness (ε_{deh}), defined as the ratio of the humidity ratio difference between the inlet and outlet air to the inlet air humidity ratio (Eq. 19), was used as a measure of performance:

$$\varepsilon_{deh} = \frac{\omega_{a,in} - \omega_{a,out}}{\omega_{a,in}} \tag{19}$$

In gas separation-based dehumidification the vacuum pump is used to compress the water vapor pressure of the feed side to equal that of the permeate side. The dehumidification COP was calculated as Eq. 20.

$$COP = \frac{\dot{Q}_{lat}}{W_{pump}} \tag{20}$$

Where $\dot{Q}_{lat}$ is the latent load removed by the vacuum membrane dehumidification system (Eq. 21), and W_{pump} is the vacuum pump's workload, obtained by Eq. 22.

$$\dot{Q}_{lat} = \dot{m}_a h_{fg} (\omega_{a,in} - \omega_{a,out}) \tag{21}$$

$$W_{pump} = \frac{\left(\frac{\dot{dm}_{mv}}{MW_{wv}} + \frac{\dot{dm}_{da}}{MW_{da}}\right) RT_k}{\varepsilon_{pump}} ln \frac{P_{atm}}{P_{vac}} \tag{22}$$

Where $\dot{dm}_{mv}$ and $\dot{dm}_{da}$ indicate the total mass flux of water vapor and dry air pumped by the vacuum pump, and the MW_{wv} and MW_{da} are the molar mass of water vapor and dry air, respectively. R is the ideal gas constant, and T_k is the absolute temperature of the inlet air. P_{atm} and P_{vac} indicate atmospheric and vacuum pressures, respectively and ε_{pump} is the vacuum pump's efficiency. In this study, vacuum pump efficiency was assumed to be 0.6.

3.1. Model validation

To validate the reliability of the proposed model, simulation results from the numerical model were compared with the experimental data from a previous study [7]. The operating ranges of the simulation conditions were set based on the valid range of each operating parameter: the inlet air temperature was varied from 25 to 33 ºC, the inlet air humidity ratio ranged from 0.012 to 0.026 kg/kg. The air flow rate was 0.067 kg/s. The permeability, selectivity, and the physical configuration of membrane dehumidifier were identical to those of the simulation model.

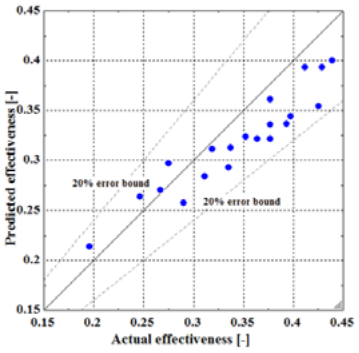

Fig. 2. Comparison of dehumidification effectiveness value with measurement data.

Figure 2 compares the dehumidification effectiveness values predicted by the proposed simulation model with the measurement data, which shows that the predicted values generally agreed well with the measurement data within 20 % error bounds. Therefore, the proposed model can be used to predict the dehumidification performance of a vacuum membrane dehumidification system.

3.2. Parametric analysis

In this section, parametric analysis was conducted to analyze the effects of variation in operating parameters on dehumidification performance of a vacuum membrane dehumidification system. The initial conditions of the four operating parameters were set as the average value in the valid range. Simulations were performed by sequentially varying each of operating parameters within the valid range, while the remaining parameters were fixed to their initial conditions. Table 1 shows the simulation conditions of each operating parameter.

Table 1. Simulation conditions of operating parameters.

Operating parameter	Range		
	Min.	Ave.	Max.
Inlet air temperature ($T_{a,in}$) [ºC]	25	30	35
Inlet air humidity ratio ($\omega_{a,in}$) [kg/kg]	0.011	0.017	0.023
Air velocity (V_a) [m/s]	0.1	1.0	2.0
Vacuum pressure (P_{vac}) [kPa]	1	5	100

Figure 3 shows the effect of each operating parameter on the dehumidification performance of a vacuum membrane dehumidification system. Air velocity (Fig. 3c) and the vacuum side pressure (Fig. 3d) significantly affected the dehumidification effectiveness and dehumidification COP, while the inlet air temperature and inlet air humidity ratio exerted minimal effect. When the vacuum side pressure increased from 1–100 kPa, the dehumidification effectiveness decreased from 55.5–2.1 % while the dehumidification COP increased from 2.15 to 23. This is because decreasing the permeate side pressure from atmospheric pressure to almost a complete vacuum can increase the water vapor difference between the feed and permeate sides, thereby increasing the driving force to remove water vapor in feed side. In terms of dehumidification COP, decreasing the vacuum side pressure had a negative effect because decreasing permeate side pressure to an almost complete vacuum imposes a large workload on the pump. Similarly, an increase in air velocity decreased the dehumidification effectiveness from 73.9 % to 15.8 %, and increased the dehumidification COP from 2.1 to 2.5. This is because the higher air velocity results in a shorter air-membrane contact time. Nevertheless, the higher air velocity increased the latent load removed by the membrane dehumidification system, which resulted in an increase of the dehumidification COP. Consequently, both dehumidification performance and COP of the vacuum membrane dehumidification system was highly affected by vacuum side pressure and inlet air velocity.

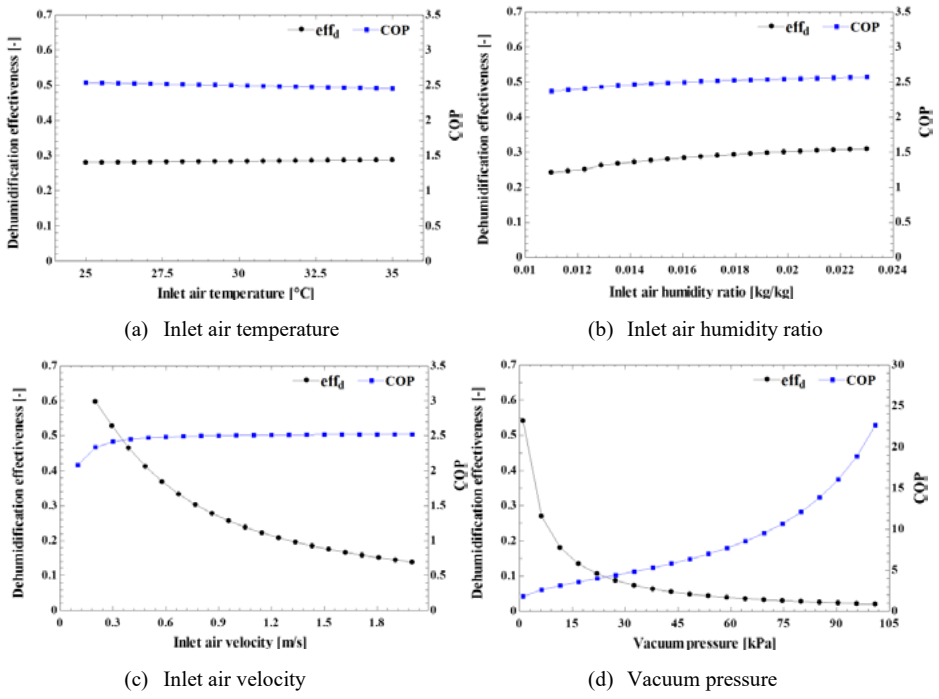

(a) Inlet air temperature (b) Inlet air humidity ratio

(c) Inlet air velocity (d) Vacuum pressure

Fig. 3. Effect of changes in operating parameters on dehumidification performance.

4. Application and discussion

In this section, energy and dehumidification performances were simulated to evaluate the operating performance of the vacuum membrane dehumidification system in HVAC applications. The design supply air flow rate was set at 200 m^3/h, which is a minimum ventilation rate for a single-story office building, located in Seoul, with 150 m^2 of floor area and eight occupants [9]. International weather for energy calculation (IWEC) data was adopted to perform the simulation for the cooling seasons in Seoul. The latent load in a model space was calculated using the TRNSYS 18 program, using the physical information of the model building (Table 2) and an office occupant and HVAC schedule addressed in ASHRAE 90.1 [10]. To maintain the supply air humidity ratio at a target point (i.e. 0.0085 kg/kg) during cooling seasons, the vacuum pump was operated to maintain the vacuum side pressure to a water vapor pressure of a target supply air (i.e. 1.19 kPa). A membrane dehumidifier with a module diameter in 0.6 m and a module length in 0.8 m was selected in order to accommodate the peak latent load during simulations.

Table 2. Physical information of the simulated building model.

Location	Seoul, Republic of Korea	
Building	15 × 10 × 3 m^3	
Heat gain	Occupants	5 persons /100 m^2
	Lights	13 W/m^2
	Computers	230 W/persons
U-value (insulation)	Exterior wall	0.524 W/m^2K

	Window	5.68 W/m^{2}K
	Roof	0.152 W/m^{2}K

4.1. Dehumidification performance

Figure 6 shows the supply air humidity ratio of the vacuum membrane dehumidification system. The performance of the dehumidifier was highly affected by the outdoor air humidity ratio. As shown in Figure 4, the supply air humidity ratio varied from 0.004 kg/kg to 0.0086 kg/kg, which demonstrated that the vacuum membrane dehumidification system can sufficiently dehumidify the outdoor air to meet the target point throughout most of the cooling seasons.

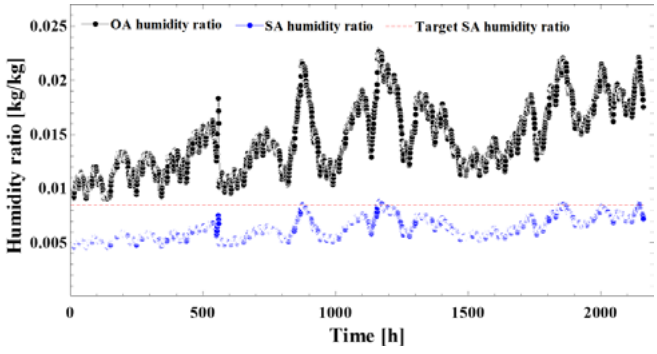

Fig. 4. Hourly supply air humidity ratio in a vacuum membrane dehumidification system.

A cooling coil was chosen as a reference system to evaluate the energy performance of the vacuum membrane dehumidification system in HVAC applications. It was assumed that the cooling coil removed the latent load to meet the supply air humidity ratio, which was the same as that of the vacuum membrane dehumidification system. Figure 5 shows the dehumidification process of a vacuum membrane dehumidification system and a conventional condensation-based dehumidification system. The vacuum membrane dehumidification system can isothermally dehumidify the outdoor air (Eq. 23), while the vapor compression system cools the outdoor air to the dew point temperature, which causes unnecessary sensible cooling (Eq. 24). Therefore, the latent cooling load for a vacuum membrane dehumidification system requires about 47 % less thermal load than that in a reference system (Fig. 6).

$$\dot{Q}_{VMD} = \dot{m}_{oa} h_{fg} (\omega_{oa} - \omega_{sa}) \tag{23}$$

$$\dot{Q}_{CC} = \dot{m}_{oa} (h_{oa} - h_{sa,dp}) \tag{24}$$

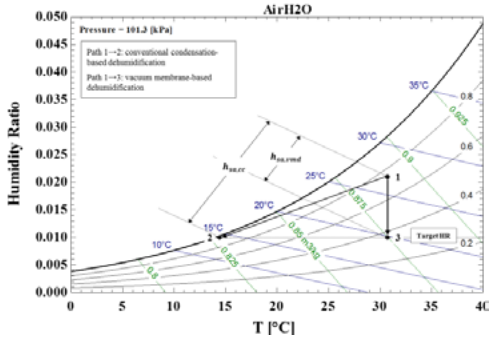

Fig. 5. Dehumidification of the proposed and reference case, presented in a psychrometric chart.

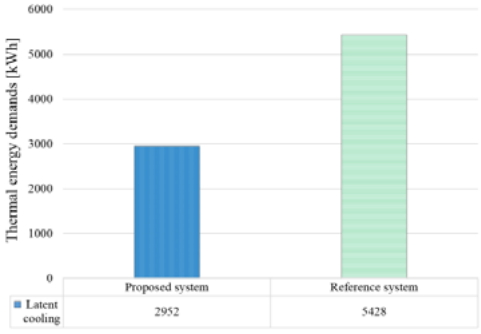

Fig. 6. Comparison of dehumidification loads.

4.2. Energy performance

Figure 8 shows that the vacuum membrane dehumidification system can reduce 47 % of the latent cooling load compared with a reference system. To evaluate the energy performance of the vacuum membrane dehumidification system, the primary energy consumption of both cases was calculated. The primary energy consumption of a vacuum membrane dehumidification system was estimated by calculating the vacuum pump operating energy with Eq. 22. The primary energy consumption of a reference system was obtained by using a chiller energy prediction model [11].

Figure 7 shows the primary energy consumption of the proposed system and reference case in cooling seasons. In contrast to the latent cooling load, the vacuum membrane dehumidification system could save only 5 % of primary energy compared to that of the reference system. This is because the dehumidification COP of a vacuum membrane dehumidifier is lower than that of the chiller. The COP of the vacuum membrane dehumidification system was maintained between 2.1 and 2.3, while that of the chiller ranged from 4.1 to 5.4. The vacuum pump should maintain the permeate side pressure to almost a complete vacuum to achieve satisfactory dehumidification, which leads to the high energy requirements of the vacuum pump. Therefore, one can conclude that the COP of the vacuum membrane dehumidification system should be improved by enhancing the dehumidification performance through a lower vacuum pump operating load.

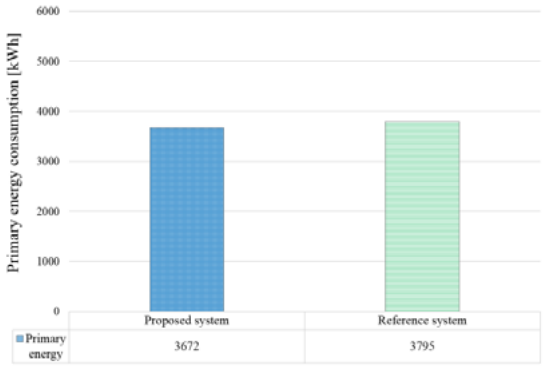

Fig. 7. Comparison of the primary energy consumption in VMD and CC

5. Conclusions

This study theoretically analyzed the dehumidification performance of a vacuum membrane dehumidification system. The governing equations for the mass flux of water vapor and dry air were derived based on the mass balance between the water vapor and dry air in the feed/permeate sides. The sensitivity of dehumidification performance on changes in operating parameters was analyzed using the proposed model. The vacuum side pressure and inlet air velocity were the most critical factors determining both dehumidification and energy performance. In particular, the dehumidification performance of a vacuum membrane dehumidification system significantly increased when the vacuum pump compressed the vacuum side pressure to equal the water vapor pressure in the inlet air.

The energy and operating performance of a vacuum membrane dehumidification system was also evaluated by comparing it with a conventional vapor compression system. The vacuum membrane dehumidification system decreased the latent cooling load by 47 % compared with a conventional cooling coil system. However, there was little energy saving potential because of the lower dehumidification COP compared to that of a reference system. Consequently, further study should consider the optimization of the vacuum pump operation strategy so that satisfactory dehumidification performance can be achieved with lower vacuum pump working loads.

Acknowledgements

This work was supported by the National Research Foundation of Korea (NRF) grant (No. 2019R1A2C2002514), the Korean Institute of Energy Technology Evaluation and Planning (KETEP) (No. 20184010201710), and the Technology development Program(S2782284) funded by the Ministry of SMEs and Startups(MSS, Korea).

References

[1] Ling, J., Hwang, Y., Radermacher, R. Theoretical study on separate sensible and latent cooling air-conditioning system, Int. J. Refrig. 2010; 33:510–520.
[2] Misha, S., Mat, S., Ruslan, M.H., Sopian, K. Review of solid/liquid desiccant in the drying applications and its regeneration methods, *Renew. Sustain. Energy Rev.* 2012; **16**:4686–4707.
[3] Woods, J. Membrane processes for heating, ventilation, and air conditioning, *Renew. Sustain. Energy Rev.* 2014; **33**:290–304.
[4] Qu, M., Abdelaziz, O., Gao, Z., Yin, H. Isothermal membrane-based air dehumidification: A comprehensive review, *Renew. Sustain. Energy Rev.* 2018; **82**:4060–4069.
[5] Bui, T.D., Wong, Y., Islam, M.R., Chua, K.J. On the theoretical and experimental energy efficiency analyses of a vacuum-based dehumidification membrane, *J. Memb. Sci.* 2017; **539**:76–87.
[6] Bui, T.D., Nida, A., Ng, K.C., Chua, K.J. Water vapor permeation and dehumidification performance of poly(vinyl alcohol)/lithium chloride composite membranes, *J. Memb. Sci.* 2016; **498**:254–262.
[7] Jang, J., Kang, E.C., Lee, H.K., Jeong, S., Park S.R. Energy demand comparison between hollow fiber membrane based dehumidification and evaporative cooling dehumidification using TRNSYS, *Energies.* 2018;**11**:1181-1196.
[8] Wang, K.L., McCray, S.H., Newbold, D.D., Cussler, E.L. Hollow fiber air drying*, J. Memb. Sci.* 1992; **72**:231–244.
[9] ASHRAE 62.1-2016 Ventilation for Acceptable Indoor Air Quality. Atlanta; 2016.
[10] ASHRAE Standard 90.1-2016. Energy standard for buildings except low-rise residential buildings. Atlanta; 2016.